filter using the LIGA micromachined process, Microwave Opt Technol Lett 30 (2001), 199–201.
10. A.A. Kachayev, D.M. Klymyshyn, S. Achenbach, and V. Saile, High vertical aspect ratio LIGA microwave 3-dB coupler, Int Conf MEMS, NANO and Smart Systems, 2003, pp. 38–43.
11. E. Mazza, S. Abel, and J. Dual, Experimental determination of mechanical properties of Ni and Ni-Fe microbars, Microsyst Technol 2 (1996), 197–202.
12. W. Sharpe, D. Lavan, and R. Edwards, Mechanical properties of LIGA-deposited nickel for MEMS, Int Conf Solid State Sensors and Actuators, 1997, pp. 607–610.
13. T. Bucheit, T. Christenson, D. Schmale, and D. Lavan, Understanding and tailoring the mechanical properties of LIGA fabricated materials, MRS Symp Proc 546 (1998), 121–126.

© 2004 Wiley Periodicals, Inc.

HIGH PERFORMANCE CPW AND MICROSTRIP RING RESONATORS ON SILICON SUBSTRATES

C. C. Chen,[1] B. F. Hung,[1] Albert Chin,[1] and S. P. McAlister[2]
[1] Institute of Electronics
National Chiao Tung University
Hsinchu, Taiwan
[2] National Research Council of Canada
Ottawa, Canada

Received 23 February 2004

ABSTRACT: *High performance CPW and novel microstrip ring resonators at ~30 GHz and 40 GHz have been fabricated on Si substrates, using an optimized proton-implantation process. Very good insertion loss and resonator characteristics, close to those from ideal electromagnetic simulations, were measured. In contrast, the ring resonators on VLSI-standard Si, without implantation, have worse transmission and reflection loss, thus prohibiting applications in RF circuits.* © 2004 Wiley Periodicals, Inc. Microwave Opt Technol Lett 42: 511–514, 2004; Published online in Wiley InterScience (www.interscience.wiley.com). DOI 10.1002/mop.20353

Key words: *CPW; ring resonators; VLSI; RF; Si*

1. INTRODUCTION

Integrated ring resonators are desirable due to their compact size, low cost, and easy fabrication. Owing to the narrow passband bandwidth and low radiation loss, ring resonators have been applied to bandpass filters, oscillators, mixers, and antennas [1–3]. Integrating a ring resonator in a CMOS circuit, on Si substrate, has advantages in producing low-cost and compact MMICs. However, the most difficult challenge in integrating such resonators is the large substrate loss from the low-resistivity Si. To overcome this problem, high-resistivity Si [4] and MEMS [5] technology have been developed. Previously, we proposed an alternative method to reduce the large RF loss from standard Si substrates using simple ion implantation, which can selectively translate the VLSI-standard Si substrates (10Ω-cm) into high resistivity material (10^6Ω-cm) [6–10]. Excellent RF passive devices such as inductors, transmission lines, filters, and antennas have been integrated into CMOS-based Si technology. In this paper, we have successfully implemented high performance 40-GHz coplanar and 30-GHz microstrip ring resonators into Si technology using ion implantation. The resonators on conventional Si, without implantation, show large insertion loss from the substrate. This is the first successful demonstration of integrated mm-wave ring resonators on Si with a process employing a VLSI-compatible technology.

2. DESIGN PROCESS

The ring resonators were designed using IE3D employing coplanar waveguide (CPW) and microstrip structures with 50Ω input impedances. The CPW structure is widely used in Si RF ICs technology because of its lower loss compared to that of microstrip-type structures. VLSI-standard Si wafers with typical 10Ω-cm resistivity were used in this study. The substrate thickness was 525 μm or 200 μm for CPW or microstrip type resonators, respectively. To reduce the RF loss from the low-resistivity Si substrate, a 1.5-μm SiO_2 layer from the VLSI backend process was first deposited. The ring resonators were fabricated on SiO_2/Si substrates using 4-μm-thick Al and standard VLSI processing for patterning. The coplanar coupled lines were laid out to form resonators, and the length (λ/2) of the coplanar resonator is dependent upon the resonant frequency. For microstrip-type resonators, 2-μm Al was also deposited on the backside of the 200-μm-thick Si, as the ground plane. Figures 1(a) and 1(b) are the images of the fabricated CPW and microstrip ring resonators designed at 40 and 30 GHz, respectively. After the ring-resonator device fabrication, ion implantation of protons was applied to reduce the RF substrate loss. The device RF characteristics were measured using an HP 8510C Network Analyzer and a probe station to 50 GHz.

3. EXPERIMENTAL RESULTS AND DISCUSSION

3.1. CPW Ring Resonator at 40 GHz

Figures 2(a) and (b) present the RF characteristics of CPW ring resonators on VLSI-standard oxide-isolated Si, with and without ion implantation, respectively. For comparison, the IE3D-designed characteristics are also shown in Figure 2(a). The implanted ring resonator has excellent RF performance, with only −1.35-dB S_{21} insertion loss at the peak transmission of 39.2 GHz and a broad ~13-GHz bandwidth. The small insertion loss is due to the large surrounding stubs being close to the ring that enhances the coupling efficiency. The measured transmission and bandwidth are close to the ring-resonator simulation, using IE3D, for an ideal lossless Si substrate. This is the first report of high performance ring resonators on Si substrates at the mm-wave regime. The merit of this ion-implantation method is its simple process and compatibility with current VLSI technology. In contrast, the ring-resonator device on the same 1.5-μm isolated Si substrate, without ion implantation, shows much worse insertion loss of 15–20 dB over the whole frequency range. Such high loss and poor resonator performance makes the devices unusable.

3.2. Thin-Film Microstrip Lines on Si

Figures 3(a) and 3(b) present the RF characteristics of the microstrip ring resonators, shown in Figure 1(b), on conventional oxide-isolated Si, with and without ion implantation, respectively. For comparison, the EM-designed characteristics from an IE3D simulation are also plotted in Figure 3(a). For the ring resonator with ion implantation, good RF performance is achieved with only −3.37-dB S_{21} insertion loss at the peak transmission of 28.3 GHz and a broad ~6-GHz bandwidth. This successful microstrip type ring resonator on Si is much more difficult to achieve than the CPW resonator because of the EM field being fully inside the lossy Si substrate. In contrast, the unimplanted microstrip ring resonators show large ~40-dB insertion loss, which prohibits their integration into any RF circuit.

3.3. Modeling and Analysis

We used a physically based equivalent-circuit model, as shown in Figure 4, to simulate the RF characteristics of the ring resonator. The shunt R_s and C_s sub-circuits simulate the substrate loss, and Cox is the parasitic oxide capacitor underneath the resonator of the 1.5-μm SiO_2 on the Si substrate. The capacitor $C1$ represents the gap-coupling capacitor, while the series L and R are the parasitic inductor and resistor, respectively, from the ring and coupling metal stub [6, 11]. The series LC forms the resonator realized by these coupling lines and the ring body. Figure 4 shows the equivalent-circuit simulated and measured RF characteristics of both the CPW and microstrip ring resonators with ion implantation. Excellent agreement between the measured and simulated S-parameters, shown in Figures 2 and 3 for both CPW and microstrip resonators, was achieved. This indicates the accuracy of the equivalent-circuit

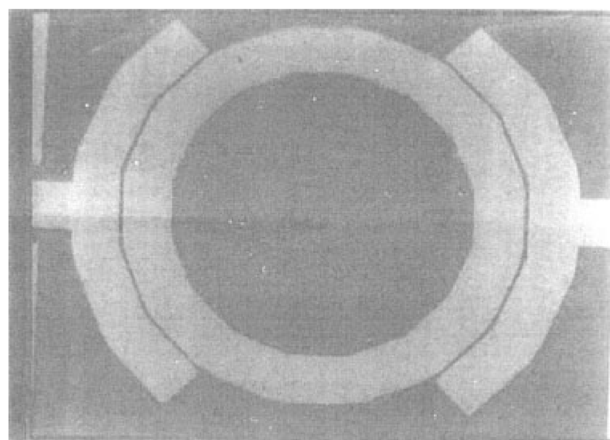

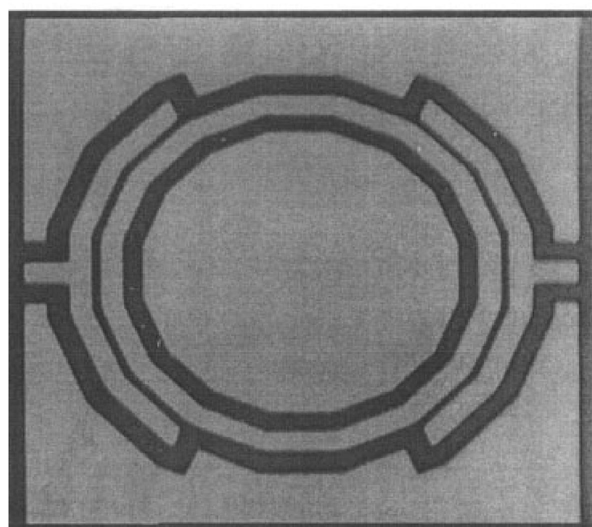

Figure 1 Images of fabricated (a) CPW and (b) microstrip ring resonators designed at 40 and 30 GHz, respectively. The long surrounded stubs near the ring are for enhancing the coupling efficiency

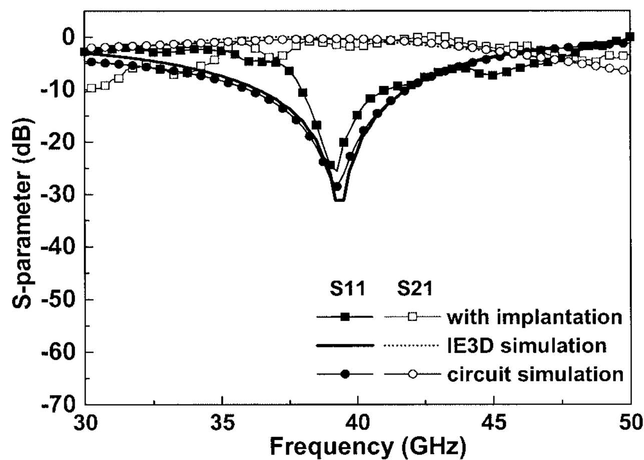

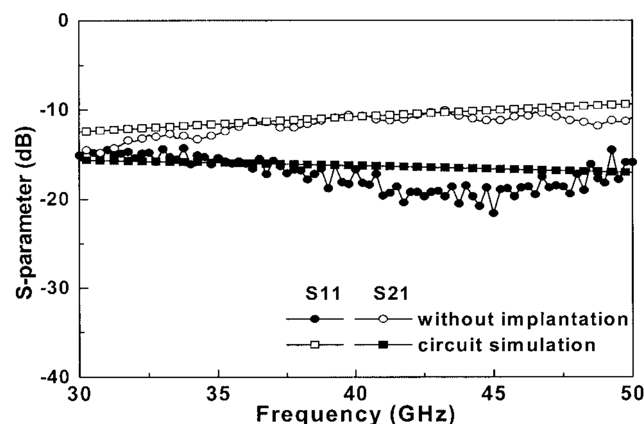

Figure 2 The measured S-parameters of CPW ring resonators (a) with and (b) without proton implantation. The EM and circuit-simulated filter characteristics are shown for reference

model. Similar good matching between the circuit-simulated and measured S-parameters was also obtained for the resonators without proton implantation in Figures 2(b) and 3(b). Thus, the equivalent circuit can be used to extract the substrate loss from Rs-Cs sub-circuits.

The extracted substrate impedance from the Rs-Cs sub-circuits is shown in Figure 5. Proton implantation increases the substrate impedances by more than an order of magnitude. The decreasing substrate impedance with increasing frequency is due to the effect of shunt capacitance to ground, which is also consistent with the higher loss at higher frequency of the transmission line and filter loss in our previous publications.

4. CONCLUSION

We have fabricated CPW and microstrip ring resonators on Si substrates with good RF performances at ~40 and ~30 GHz, close to that for ideal IE3D-designed resonators. This was achieved using proton implantation. Without implantation, such resonators have worse insertion and reflection losses and completely fail. By using equivalent-circuit models and EM simulation, we conclude that substrate impedances are the major cause of the poor RF performance.

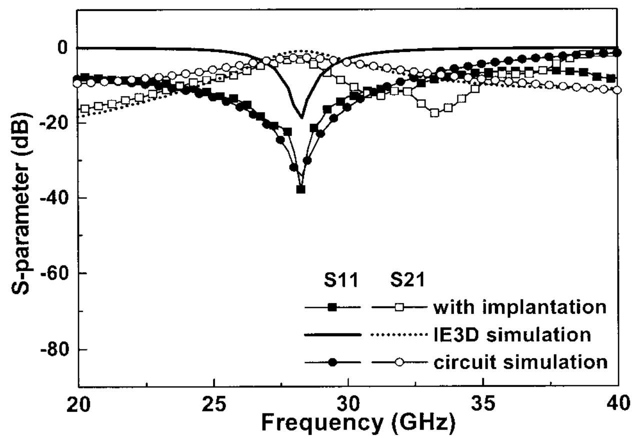

(a)

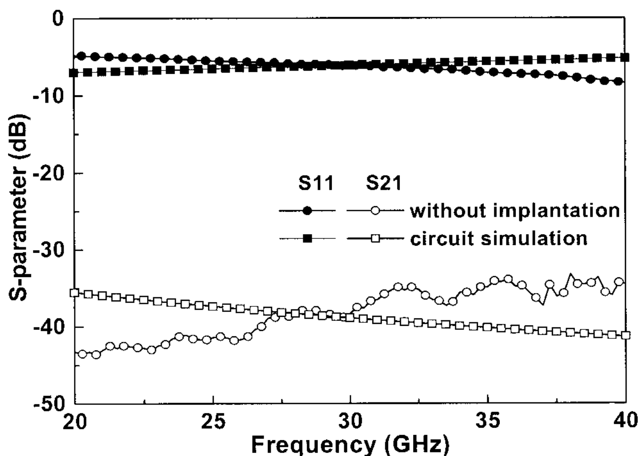

(b)

Figure 3 The measured S-parameters of 30-GHz microstrip line ring resonators (a) with and (b) without proton implantation. The EM-simulated and equivalent circuit-simulated filter characteristics are also shown for reference. No resonance is observed in (b) due to the substrate loss of ~40 dB

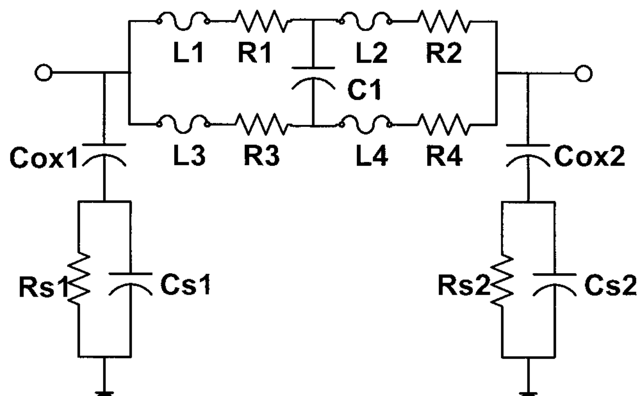

Figure 4 Physically based equivalent circuit of the ring resonators. L expresses the metal stub, and C_1 is the fringing coupling capacitance of the ring. The substrate loss is modeled by the shunt R_s and C_s to ground

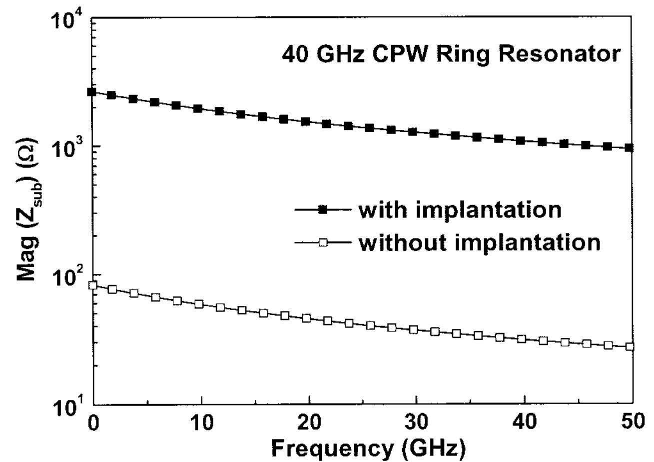

(a)

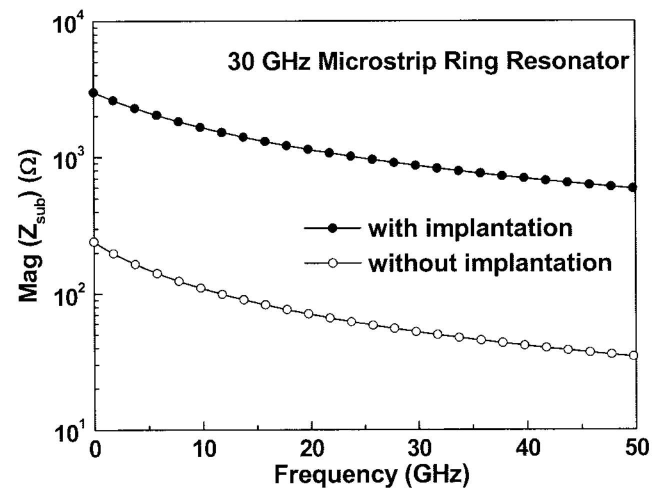

(b)

Figure 5 Extracted magnitude of the substrate impedance from (a) CPW ring resonators and (b) microstrip ring resonators with or without implantation. The substrate impedances were increased by the implantation, thus reducing the insertion loss of the ring resonators

ACKNOWLEDGMENTS

We would like to thank Dr. G. W. Huang at NDL for helping with the measurements. This work has been supported by NSC (92-2215-E-009-017).

REFERENCES

1. K. Chang, Microwave ring circuits and antennas, Wiley, New York, 1996.
2. L. Zhu, and K. Wu, A joint field/circuit model of line-to-ring coupling structures and its application to the design of microstrip dual-mode filters and ring resonator circuits, IEEE Trans Microwave Theory Tech 47 (1999), 1938–1948.
3. H. Yabuki, M. Sagawa, M. Matsuo, and M. Makimoto, Stripline dual-mode ring resonators and their application to microwave devices, IEEE Trans Microwave Theory Tech 44 (1996), 723–729.
4. T. Ohguro, K. Kojima, H.S. Momose, S. Nitta, T. Fukuda, T. Enda, and Y. Toyoshima, Improvement of high resistivity substrate for future mixed analog-digital application, VLSI Tech Symp Dig (2002), 158–159.
5. E.C. Park, S.H. Baek, T.S. Song, J.B. Yoon, and E. Yoon, Performance

comparison of 5GHz VCOs integrated by CMOS compatible high Q MEMS inductors, IEEE MTT-S Int Microwave Symp Dig (2003), 721–724.
6. K.T. Chan, A. Chin, J.T. Kuo, C.Y. Chang, D.S. Duh, W.J. Lin, C.X. Zhu, M.F. Li, and D.L. Kwong, Microwave coplanar filters on Si substrates, IEEE MTT-S Int Microwave Symp (2003), 1909–1912.
7. K.T. Chan, A. Chin, C.M. Kwei, D.T. Shien, and W.J. Lin, Transmission line noise from standard and proton-implanted Si, IEEE MTT-S Int Microwave Symp Dig (2001), 763–766.
8. K.T. Chan, A. Chin, Y.B. Chen, Y.-D. Lin, D.T.S. Duh, and W.J. Lin, Integrated antennas on Si, proton-implanted Si and Si-on-quartz, Int Electron Devices Mtg (IEDM) Tech Dig (2001), 903–906.
9. Y.H. Wu, A. Chin, K.H. Shih, C.C. Wu, S.C. Pai, C.C. Chi, and C.P. Liao, RF loss and cross talk on extremely high resistivity (10K-1M-cm) Si fabricated by ion implantation, IEEE MTT-S Int Microwave Symp Dig (2000), Boston, MA, 241–244.
10. A. Chin, K. Lee, B.C. Lin, and S. Horng, Picosecond photoresponse of carriers in Si ion-implanted Si, Appl Phys Lett 69 (1996), 653–656.
11. K. Hettak, N. Dib, A.F. Sheta, and S. Toutain, A class of novel uniplanar series resonators and their implementation in original applications, IEEE Trans Microwave Theory Tech 46 (1998), 1270–1276.

© 2004 Wiley Periodicals, Inc.

5.2-GHz SUBHARMONIC INJECTION-LOCKED DISTRIBUTED OSCILLATOR

Chung Ming Yuen and Kim Fung Tsang
Department of Electronic Engineering
City University of Hong Kong
Tat Chee Avenue, Kowloon
Hong Kong SAR, P.R. China

Received 21 February 2004

ABSTRACT: *A novel subharmonic injection-locked distributed oscillator is proposed and presented. A 5.2-GHz distributed oscillator is locked to a 2.6-GHz injection source. The injection source is applied to the feedback path between the collector line and the base line of the distributed oscillator for optimal locking range. The circuit is designed for 2.7-V operation. The developed oscillator delivers +3-dBm output power with a phase noise of −110 dBc/Hz at 500-kHz offset at 5.2 GHz.* © 2004 Wiley Periodicals, Inc. Microwave Opt Technol Lett 42: 514–516, 2004; Published online in Wiley InterScience (www.interscience.wiley.com). DOI 10.1002/mop.20354

Key words: *injection-locked oscillator; distributed oscillator*

1. INTRODUCTION

In microwave-oscillator design, it is difficult to achieve high output power with low-phase noise under low voltage. Such difficulty will be more profound when the oscillating frequency approaches the cutoff frequency of the active device due to the decrease of the gain and the increase of noise of the active device. It was well documented that the distributed oscillator [1] has the advantage of wide tuning range and high output power. In 1998, Divina et al. [2] successfully implemented a 4-GHz distributed oscillator using four discrete PHEMTs. Usually a distributed oscillator does not provide good phase noise, especially when the dc drive is under low voltage. In this paper, we apply the injection-locking technique to a distributed oscillator in order to achieve a high-power but low-noise microwave oscillator. The use of the subharmonic injection-locking technique manifests good phase-noise signals at higher frequency by injection locking to a highly stable lower-frequency signal [3]. It was also reported by Lee and Hong that a wide locking range could be achieved for microwave-frequency synthesis and modulation by using the injection-locking technique [4]. This paper shows the successful application of injection-locking technique to a 5.2-GHz distributed oscillator in order to achieve high output power and low-phase noise. The oscillator was designed and implemented to realize wireless LAN applications in the 5-GHz band.

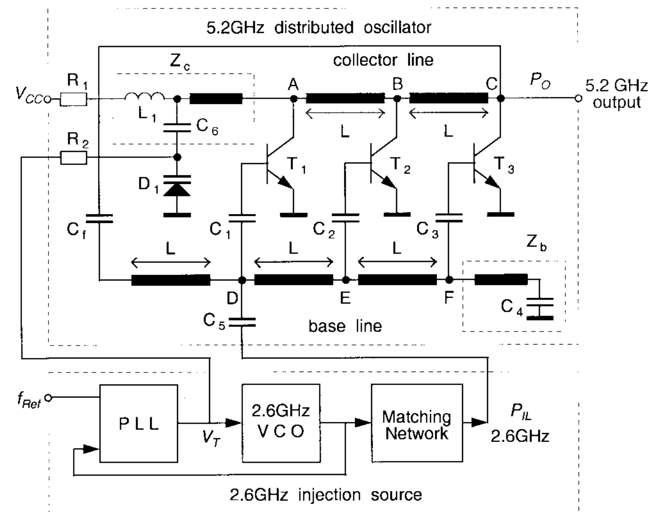

Figure 1 Injection-locked distributed oscillator

2. DESIGN OF INJECTION-LOCKED DISTRIBUTED OSCILLATOR

The simplified (without biasing) injection-locked distributed oscillator (ILDO) is illustrated in Figure 1. The upper block shows a 5.2-GHz distributed oscillator, which is based on a three-stage distributed amplifier. The distributed oscillator utilizes the forward-gain mode of a distributed amplifier. Adopting a similar analysis by Wu and Hajimiri [5], the forward wave on the base line is amplified by each transistor and appears on the collector line. The signal on the collector line travels forward in synchronization with the traveling wave on the base line. The signal from each transistor adds constructively at each tapping point on the collector line. Thus, the forward path has an overall gain that is much larger than unity, while the gain of each transistor stage may be small. Oscillation is created by connecting the amplifier output back to the input through the feedback capacitor C_f. The signals building up the oscillation will experience a delay, including the delay around the loop plus the delay between base-to-collector. In order to minimize reflection, the collector line and the base line are terminated by loads Z_c and Z_b, respectively. There are five identical transmission line sections: two sections (A-B and B-C) on the collector line, two sections (D-E and E-F) on the base line, and one section (C-D) on the feedback path. To fulfill the oscillation condition at the target frequency, the phase shift between the collector and the base of each transistor must satisfy $\theta = n\lambda/2$ (where $n = 1, 3, 5, \ldots$; λ = guided wavelength). It was found that $n = 1$ yielded the best noise performance. Hence, $L = \lambda/6$ was selected. For 5.2-GHz oscillation frequency, the length of L was calculated to be 3.9 mm for a dielectric constant of 4.2. In our implementation, the collectors were dc-coupled to the collector line and biased by a single current source while the bases of the transistors were ac-coupled to the base line by capacitors C_1, C_2, and C_3. The base-biasing voltage fed each transistor individually.